Inorganic Chemistry

Article

pubs.acs.org/IC

Synthesis and Structure of Six-Coordinate Iron Borohydride Complexes Supported by PNP Ligands

Ingo Koehne,[†,‡] Timothy J. Schmeier,[‡,§] Elizabeth A. Bielinski,[§] Cassie J. Pan,[§] Paraskevi O. Lagaditis,[†] Wesley H. Bernskoetter,[⊥] Michael K. Takase,[§] Christian Würtele,[†] Nilay Hazari,*[,§] and Sven Schneider*[,†]

[†]Institut für Anorganische Chemie, Georg-August-Universität Göttingen, Tammannstrasse 4, 37077 Göttingen, Germany

[§]Department of Chemistry, Yale University, P.O. Box 208107, New Haven, Connecticut 06520, United States

[⊥]Department of Chemistry, Brown University, Providence, Rhode Island 02912, United States

Supporting Information

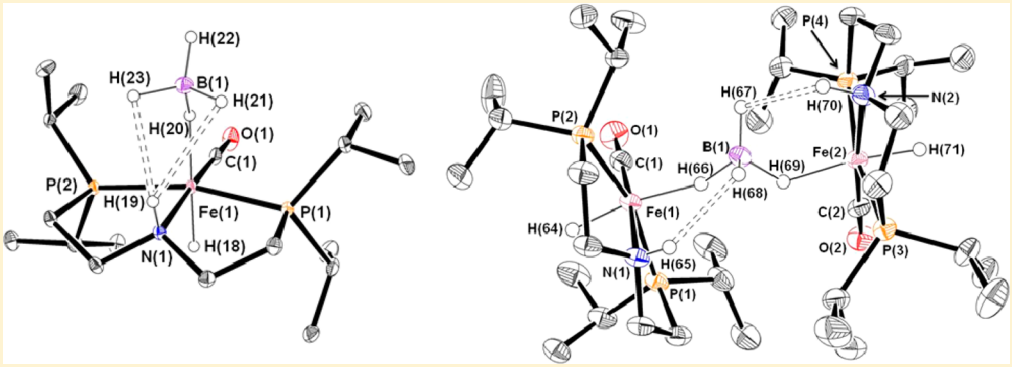

ABSTRACT: The preparation of a number of iron complexes supported by ligands of the type $HN\{CH_2CH_2(PR_2)\}_2$ [R = isopropyl (^{iPr}PNP) or cyclohexyl (^{Cy}PNP)] is reported. This is the first time this important bifunctional ligand has been coordinated to iron. The iron(II) complexes (^{iPr}PNP)$FeCl_2(CO)$ (**1a**) and (^{Cy}PNP)$FeCl_2(CO)$ (**1b**) were synthesized through the reaction of the appropriate free ligand and $FeCl_2$ in the presence of CO. The iron(0) complex (^{iPr}PNP)$Fe(CO)_2$ (**2a**) was prepared through the reaction of $Fe(CO)_5$ with ^{iPr}PNP, while irradiating with UV light. Compound **2a** is unstable in CH_2Cl_2 and is oxidized to **1a** via the intermediate iron(II) complex [(^{iPr}PNP)$FeCl(CO)_2$]Cl (**3a**). The reaction of **2a** with HCl generated the related complex [(^{iPr}PNP)$FeH(CO)_2$]Cl (**4a**), while the neutral iron hydrides (^{iPr}PNP)FeHCl(CO) (**5a**) and (^{Cy}PNP)FeHCl(CO) (**5b**) were synthesized through the reaction of **1a** or **1b** with 1 equiv of $^{n}Bu_4NBH_4$. The related reaction between **1a** and excess $NaBH_4$ generated the unusual η^1-HBH_3 complex (^{iPr}PNP)$FeH(\eta^1$-$HBH_3)(CO)$ (**6a**). This complex features a bifurcated intramolecular dihydrogen bond between two of the hydrogen atoms associated with the η^1-HBH_3 ligand and the N−H proton of the pincer ligand, as well as intermolecular dihydrogen bonding. The protonation of **6a** with 2,6-lutidinium tetraphenylborate resulted in the formation of the dimeric complex [{(^{iPr}PNP)$FeH(CO)$}$_2(\mu_2,\eta^1{:}\eta^1$-$H_2BH_2)$][BPh_4] (**7a**), which features a rare example of a $\mu_2,\eta^1{:}\eta^1$-H_2BH_2 ligand. Unlike all previous examples of complexes with a $\mu_2,\eta^1{:}\eta^1$-H_2BH_2 ligand, there is no metal−metal bond and additional bridging ligand supporting the borohydride ligand in **7a**; however, it is proposed that two dihydrogen-bonding interactions stabilize the complex. Complexes **1a**, **2a**, **3a**, **4a**, **5a**, **6a**, and **7a** were characterized by X-ray crystallography.

INTRODUCTION

Since Shaw and co-workers[1] described the first examples of pincer-supported transition-metal complexes in the 1970s, these ligands have become ubiquitous in modern coordination and organometallic chemistry.[2] There are two major reasons why pincer ligands are commonly used: (i) They often have relatively easy and modular syntheses, which allow facile tuning of the steric and electronic properties of the resulting transition-metal complexes. (ii) The rigid binding of the ligand to three coplanar sites of the metal frequently generates complexes with extremely high thermal stability. In recent years, bifunctional pincer-type ligands, such as the tridentate chelating PNP ligand $HN(CH_2CH_2PR_2)_2$ (^{R}PNP; R = alkyl or aryl), have received significant attention and have been coordinated to a variety of different transition metals.[3] These ligands have been used both to stabilize transition-metal catalysts and to support complexes in unusual geometries. For example, Beller and co-workers[3ad] have catalytically dehydrogenated methanol to H_2 and CO_2 using a ruthenium complex

Received: November 4, 2013

   dx.doi.org/10.1021/ic402762v | Inorg. Chem. XXXX, XXX, XXX−XXX

supported by a ^{R}PNP ligand, while some of us utilized ligands of this type to stabilize electron-rich nitrido complexes of ruthenium, rhodium, and iridium.[3x,z,ac] A particularly striking feature of ^{R}PNP ligands is that they can participate in reactions that involve metal−ligand cooperativity.[3e,o−q,s,w] In fact, both the N−H bond and one of the C−H bonds of the ethylene linker can be reversibly activated.[3p,w] As a result, these types of ligands have been utilized to support transition-metal catalysts, which operate via a bifunctional mechanism, for both the hydrogenation and transfer hydrogenation of polar double bonds and the dehydrogenation of boraneamines.[3e,o−q,s,w,ab]

Despite the many examples of bifunctional catalysis with ruthenium species supported by ^{R}PNP pincer ligands,[3i,q,s,w,ab,ad] analogous iron chemistry has been neglected. In fact, to date, there have been no reports of iron complexes stabilized by ^{R}PNP ligands.[4] This is even more surprising given that related ligands have been successfully utilized in iron-catalyzed transformations. For example, Morris and co-workers employed iron complexes supported by bifunctional tetradentate PNNP-type ligands as highly efficient catalysts for the transfer hydrogenation of ketones,[5] while Milstein and co-workers reported that pincer complexes such as {2,6-C_5H_3N-$(CH_2P^iPr_2)_2$}FeH(η^1-HBH_3)(CO) are active catalysts for the base-free hydrogenation of ketones.[6] It should be noted that apart from its catalytic applications, Milstein's borohydride complex is also important because it represents a rare example of an iron species with an η^1-borohydride (BH_4^-) ligand.[6b,7] In general, of the three coordination modes (η^1, η^2, and η^3; Figure 1a) that have been described for mononuclear borohydride complexes,[8] the η^2-binding mode is the most commonly found,[8] while η^1-coordination is relatively unusual, especially for d^6 metal ions.[6b,7,9] Even in the few reported examples of dinuclear complexes with bridging borohydride ligands, the $\mu_2,\eta^2:\eta^2$-H_2BH_2-coordination mode (Figure 1b) is by far the most common,[10] and there are only two examples of complexes with bridging $\mu_2,\eta^1:\eta^1$-H_2BH_2 ligands.[11] In both of these cases, the complexes also contain a supporting metal−metal bond and bridging hydride ligand.

Given our interest in the coordination chemistry of complexes with bifunctional ligands, here we report the synthesis of iron complexes with ^{R}PNP ligands [R = isopropyl (^{i}Pr) or cyclohexyl (Cy)]. In particular, we have prepared a number of complexes that feature unusual binding modes of borohydride ligands, including a dimeric species with a bridging $\mu_2,\eta^1:\eta^1$-H_2BH_2 ligand, which does not contain a metal−metal bond or a bridging hydride ligand. All of our borohydride-containing species contain interesting examples of dihydrogen bonds, which stabilize the complexes.[12]

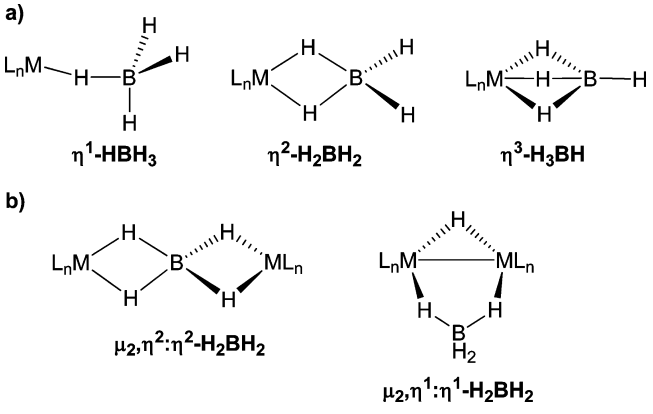

Figure 1. Reported coordination modes of borohydride ligands in (a) monomeric and (b) dimeric complexes.

RESULTS AND DISCUSSION

Metalation of the Ligand. Two routes were evaluated for the preparation of Fe(PNP) complexes, starting from iron(0) ($Fe(CO)_5$) and iron(II) ($FeCl_2$) precursors, respectively. The treatment of $FeCl_2$ with either ^{iPr}PNP or ^{Cy}PNP, followed by the addition of CO, results in the formation of the six-coordinate iron(II) complexes (^{iPr}PNP)$FeCl_2$(CO) (**1a**) and (^{Cy}PNP)$FeCl_2$(CO) (**1b**), respectively, in yields of at least 70% (eq 1). This is a synthetic route analogous to that described by Milstein et al. for the coordination of the pyridine-based ligand 2,6-$C_5H_3N(CH_2P^iPr_2)_2$ to $FeBr_2$.[6a] The reaction is considerably slower for the ^{Cy}PNP ligand (4 h at 50 °C) compared to the ^{iPr}PNP ligand (2 h at room temperature), presumably because of the increased steric bulk of the cyclohexyl ligand. The strong-field ligand CO was introduced to ensure a low-spin ground-state configuration.[13] Accordingly, the new complexes are diamagnetic, and a single sharp resonance is observed at 67.9 ppm in the $^{31}P\{^1H\}$ NMR spectrum of **1a** while the corresponding peak in the spectrum of **1b** is observed at 58.9 ppm. The IR spectra of **1a** and **1b** contain strong CO stretching vibrations at 1926 and 1944 cm^{-1}, respectively, while the N−H stretches are located at 3203 and 3188 cm^{-1}, respectively. Surprisingly, when $FeCl_2$ was treated with the even more sterically bulky ^{tBu}PNP ligand, followed by the addition of CO, there was no evidence for the formation of a diamagnetic species equivalent to **1a** or **1b**. Given the similar electronic properties of the isopropyl, *tert*-butyl, and cyclohexyl substituents, we propose that this is due to steric factors. The molecular structure of **1a**, which was elucidated by X-ray diffraction, is shown in Figure 2, and important bond distances and angles are summarized in Table 1. The iron atom is located within a distorted octahedral coordination geometry, and the chloride ligands occupy mutually *trans* positions. The ^{iPr}PNP ligand is coordinated meridionally with the CO ligand *trans* to the ^{iPr}PNP nitrogen donor. There are two independent molecules in the unit cell, and the P(1)−Fe(1)−P(2) and Cl(1)−Fe(1)−Cl(2) bond angles of 168.96(4) and 168.82(4)° and 173.44(3) and 172.68(11)°, respectively, are indicative of the distorted octahedral geometry around the iron center. The Fe(1)−N(1) bond distances in the two independent molecules [2.065(2) and 2.071(3) Å] are consistent with other Fe−amine bonds.[6a,14] Overall, the bond distances and angles of **1a** are similar to those observed in the related compounds *trans*-(^{iPr}PNP)$RuCl_2(PMe_3)$[3w] and {2,6-$C_5H_3N(CH_2P^iPr_2)_2$}-$FeBr_2$(CO).[6a] For example, the (^{iPr}PNP)Ru complex exhibits a comparable Cl−Ru−Cl bond angle [171.04(2)°], yet a slightly smaller P−Ru−P bite angle [163.04(3)°] as a consequence of the longer Ru−N bond length [2.113(4) Å].

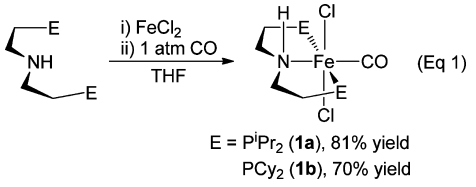

E = P^{i}Pr$_2$ (**1a**), 81% yield
PCy$_2$ (**1b**), 70% yield

dx.doi.org/10.1021/ic402762v | *Inorg. Chem.* XXXX, XXX, XXX−XXX

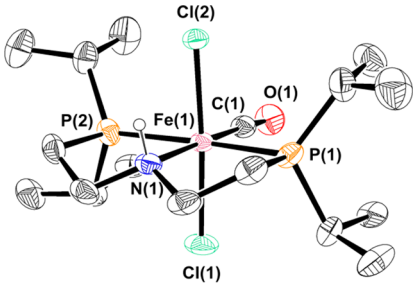

Figure 2. ORTEP of **1a** at 50% probability. Selected hydrogen atoms have been omitted for clarity, and only one of the two independent molecules in the unit cell is shown.

An alternative preparative route to **1a** starts from $Fe(CO)_5$. Irradiation in the presence of $^{i\text{Pr}}$PNP in acetone results in the formation of the diamagnetic five-coordinate iron(0) complex ($^{i\text{Pr}}$PNP)$Fe(CO)_2$ (**2a**; Scheme 1), which was isolated and fully characterized. A single resonance at 109.8 ppm is observed in the $^{31}P\{^1H\}$ NMR spectrum of **2a**. The two separate peaks at 222.4 and 226.2 ppm in the $^{13}C\{^1H\}$ NNR spectrum of **2a** can be assigned to chemically inequivalent CO ligands, which is in agreement with the two CO stretching vibrations observed by IR spectroscopy (1838 and 1767 cm^{-1}). The significant decrease in the average CO stretching frequency in the iron(0) complex **2a**, compared with the iron(II) complexes **1a** and **1b**, is consistent with an increase in the back-donation to the CO ligands from the more electron-rich metal center in the lower oxidation state. The molecular structure of **2a**, obtained by X-ray diffraction (Figure 3), reveals a square-pyramidal geometry around the iron atom. The PNP ligand is bound meridionally and occupies three positions of the base of the square pyramid, while the two CO ligands occupy the remaining basal position and the apical position. This is consistent with two different resonances being observed for the carbonyl ligands in the ^{13}C NMR spectrum, with slow or no exchange of these ligands on the NMR time scale at room temperature. The P(1)−Fe(1)−P(2) bond angle in **2a** [158.58(2)°] is smaller than that in **1a**, presumably as a consequence of the change in the geometry of the complex from octahedral in **1a** to square-pyramidal in **2a**. As a result, the Fe(1)−N(1) bond distance is longer in **2a** [2.1281(12) Å] than in **1a**.

Complex **2a** is oxidized upon dissolution in dichloromethane (Scheme 1). The solution initially changes from dark green to pale yellow, and after 12 h, a reddish-brown solution is observed. NMR spectroscopy indicates that the purple dichloride complex **1a** is the major product. Although relatively high spectroscopic yields of **1a** were detected, this complex could only be isolated in approximately 25% yield, presumably because of loss during purification by column chromatography. When the reaction was monitored by $^{31}P\{^1H\}$ NMR spectroscopy, several reaction intermediates, which could not be characterized, were observed. However, a crystallization attempt after partial conversion resulted in the isolation of a crystal of the iron(II) dicarbonyl complex [($^{i\text{Pr}}$PNP)FeCl-$(CO)_2$]Cl (**3a**), which was only characterized by X-ray crystallography.[15] This suggests that oxidation of **2a** by the solvent proceeds through the dicarbonyl intermediate **3a**, which loses CO over time to form **1a** (Scheme 1). Nevertheless, the considerably lower overall yield renders direct synthesis of **1a** from $FeCl_2$, $^{i\text{Pr}}$PNP, and CO our preferred route.

Preparation of Hydride-Containing Complexes. The reaction of **2a** with HCl results in the protonation of the iron(0) complex and the formation of the six-coordinate iron(II) cation [($^{i\text{Pr}}$PNP)$FeH(CO)_2$]Cl (**4a**), with a chloride counterion (eq 2). **4a** exists as a mixture of two isomers, as evidenced by two sets of signals in the NMR spectra (for example, in the $^{31}P\{^1H\}$ NMR spectrum, two signals are observed at 99.5 and 102.1 ppm). The ratio of these signals is always 3:1 at room temperature and does not vary between independent preparations of **4**. Both sets of signals are consistent with meridional coordination of the $^{i\text{Pr}}$PNP ligand and the hydride in a *trans* position to a CO ligand, as judged by their ^1H NMR chemical shifts (−7.38 and −8.22 ppm). Given the similar NMR chemical shifts between the two isomers, we propose that the two structures have either *cis*- or *trans*-coplanar arrangements of the N−H and Fe−H moieties, respectively, as shown in eq 2. Further confirmation of this assignment was obtained through X-ray crystallography because the structure of $\mathbf{4a}^{\text{Trans}}$ was elucidated.[15] NMR spectroscopy on the single crystals used for X-ray crystallography allowed us to determine that $\mathbf{4a}^{\text{Trans}}$ is the main product of the reaction. The CO stretching vibrations are observed at 1998 and 1943 cm^{-1} for $\mathbf{4a}^{\text{Trans}}$ and at 1987 and 1932 cm^{-1} for $\mathbf{4a}^{\text{Cis}}$ in the IR spectrum, consistent with the stretching frequencies observed in the other iron(II) complexes synthesized as part of this work. Presumably, a geometry with the hydride *trans* to the CO ligand, as opposed to *trans* to the nitrogen atom of the PNP ligand, is favored because it leads to less competition between the two CO ligands for the electron density from the iron center for back-donation.The neutral iron(II) hydridochloride complexes **5a** and **5b** were obtained through the reaction of **1a** or **1b** with 1 equiv of $^n\text{Bu}_4\text{NBH}_4$ in acetonitrile (ACN) at room temperature, followed by recrystallization at −30 °C (Scheme 2). The related reactions between **1a** and **1b** and 1 equiv of

Table 1. Selected Bond Distances (Å) and Angles (deg) for the ($^{i\text{Pr}}$PNP)Fe Complexes 1a, 2a, 5a, 6a, and 7a

compound	Fe(1)−N(1)	Fe(1)−C(1)	Fe(1)−X(1)	Fe(1)−X(2)	C(1)−O(1)	P(1)−Fe(1)−P(2)
1a[a]	2.065(2) and 2.071(3)	1.743(4) and 1.753(4)	2.3201(9) and 2.322(2); X = Cl	2.3417(10) and 2.331(1); X = Cl	1.133(4) and 1.1458(5)	168.96(4) and 168.82(4)
2a[b]	2.1281(12)	1.7188(15)^{ba}, 1.7449(15)^{ax}			1.1809(19)^{ba}, 1.1848(17)^{ax}	158.58(2)
5a	2.070(3)	1.713(4)	2.4125(10); X = Cl	1.43(3); X = H	1.161(4)	165.01(4)
6a	2.0715(13)	1.723(6)	1.707(18); X = η^1-HBH_3	1.45(2); X = H	1.170(6)	165.920(18)
7a	2.074(2)	1.720(3)	1.74(2); X = μ_2, η^1:η^1-HBH_3	1.47(2); X = H	1.169(3)	163.74(3)

[a]There are two independent molecules in the unit cell. [b]**2a** has two CO ligands: ba refers to the CO that is part of the base of the square pyramid, and ax refers to the CO that is in the axial position.

dx.doi.org/10.1021/ic402762v | Inorg. Chem. XXXX, XXX, XXX−XXX

Scheme 1

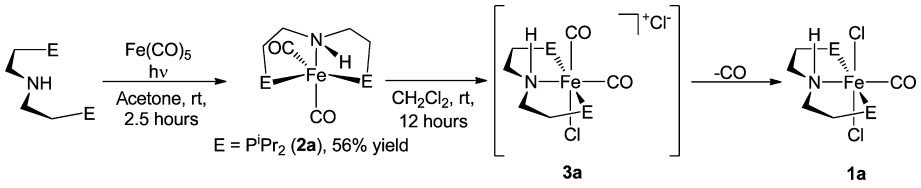

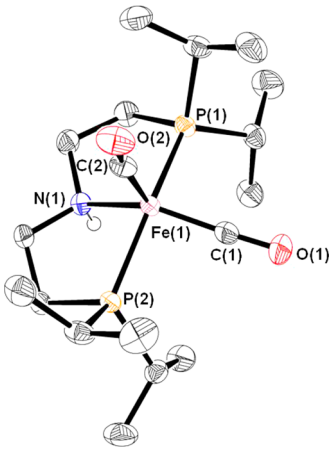

Figure 3. ORTEP of **2a** at 50% probability. Selected hydrogen atoms have been omitted for clarity.

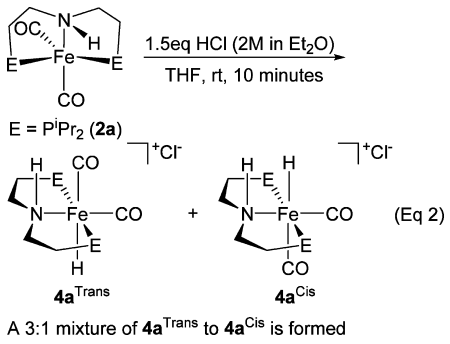

(Eq 2)

$NaBH_4$ give a mixture of products, while the reaction of **1a** with $LiHBEt_3$ also gave clean conversion to **5a** (in higher yield than the corresponding $^nBu_4NBH_4$ reaction; see the Experimental Section). This indicates that the choice of the hydride source is crucial and Kemp, Goldberg, and co-workers have previously made similar observations while preparing Ni–H species supported by pincer ligands.[16] Complex **5a** could also be prepared by photodecarbonylation of **4a** with UV light (Scheme 2); however, isolated yields were lower than those of the direct synthesis from **1a** because of the need for purification using column chromatography. The metal hydride resonances of **5a** and **5b** appear as triplets at −19.1 and −19.4 ppm, respectively, in the ^1H NMR spectrum. The N–H stretching frequencies for the PNP ligands in the solid-state IR spectra of **5a** and **5b** were located at 3183 and 3134 cm^{-1}, respectively. This shift to lower frequency compared to the dichloride complexes **1a** and **1b** is consistent with the formation of a hydrogen bond involving the N–H bond of the ligand. For example, the observed stretching frequency in **5a** is quite similar to the N–H stretching frequency in a (^{iPr}PNP)Ir^{III} formate complex that we have reported previously, which contains an N–H···(O)CHOIr hydrogen bond.[3o] The CO stretching frequencies of both **5a** (1895 cm^{-1}) and **5b** (1895 cm^{-1}) are significantly lower than those in **1a** and **1b**, which is consistent with the hydride ligand being a better σ donor than the chloride ligand.[17] In the case of complexes **5a** and **5b**, no nuclear Overhasuer effect (NOE) was observed between the N–H proton and Fe–H by ^1H NMR spectroscopy, and on that basis, we propose that the N–H proton is located in the *trans* position with respect to the hydride ligand.

When the reaction of **1a** and $^nBu_4NBH_4$ was monitored by ^1H and ^{31}P NMR spectroscopy the formation of two products in a 6:1 ratio was initially observed, with **5a** being the minor species (Scheme 3). This product mixture eventually converted exclusively to **5a** upon standing in solution, with no intermediates detected. The initially formed major product showed a clear triplet at −18.6 ppm in the ^1H NMR spectrum, which integrated to one proton. This is consistent with the presence of a single Fe–H bond. A singlet was observed at 96.3 ppm in the $^{31}P\{^1H\}$ NMR spectrum, which is quite close to the $^{31}P\{^1H\}$ NMR chemical shift observed for **5a** (95.4 ppm). At this stage, we propose that the initially formed product is an isomer of **5a** in which the N–H and Fe–H moieties are oriented *cis* with respect to each other (**5a**^{Cis}). Our hypothesis is that the ligand substitution of **1a** with $^nBu_4NBH_4$ is kinetically controlled and a diastereomeric product mixture is initially obtained because the hydride can attack either of the two faces containing the chloride ligands in **1a**. However, instead of an initial statistical 1:1 ratio of the isomers **5a**^{Cis} and **5a**, a 6:1 ratio of **5a**^{Cis} and **5a** is observed because of the directing ability of the N–H moiety. Intermolecular dihydrogen bonding[12] between $^nBu_4NBH_4$ and the N–H bond of the PNP ligand in **1a** would favor hydride delivery to form **5a**^{Cis}. Subsequent isomerization of **5a**^{Cis} to **5a** gives exclusively one product, although at this stage, the pathway for isomerization is

Scheme 2

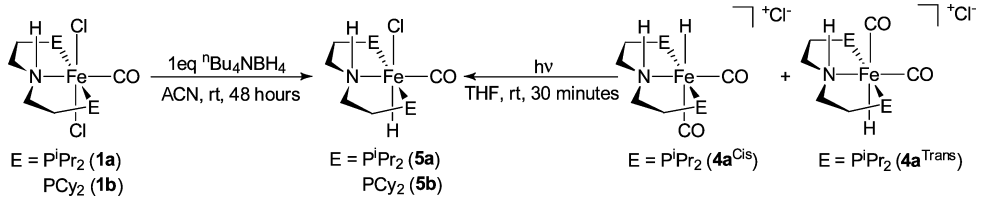

dx.doi.org/10.1021/ic402762v | Inorg. Chem. XXXX, XXX, XXX–XXX

Scheme 3

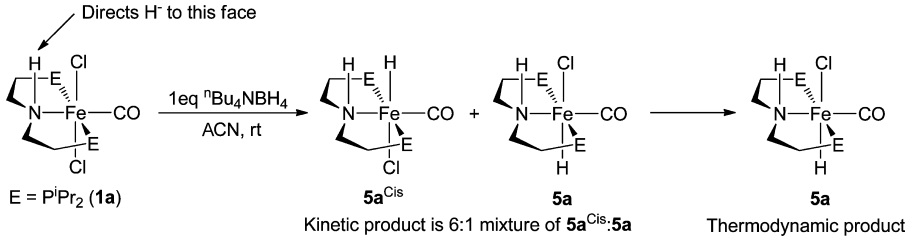

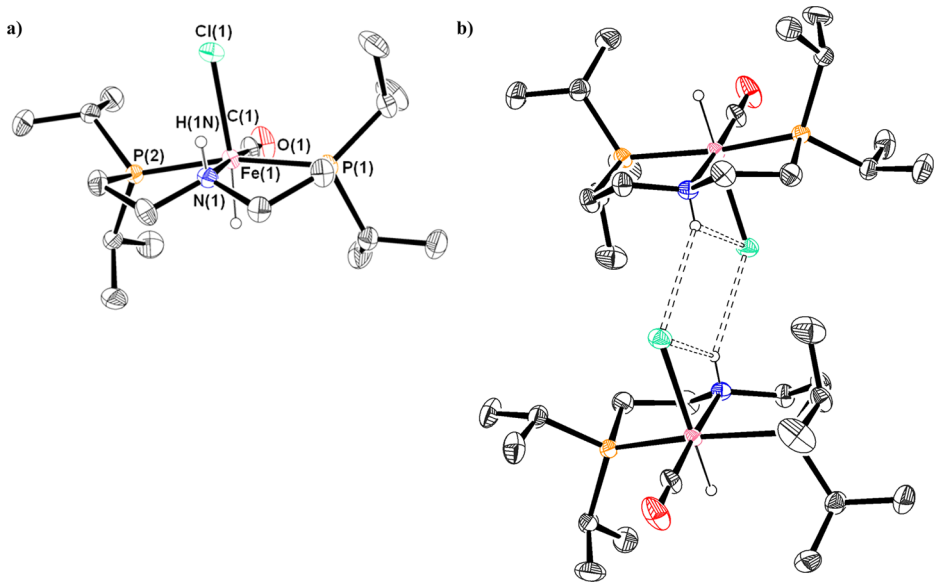

Figure 4. (a) ORTEP of **5a** at 50% probability. (b) Dimeric packing of **5a** at 50% probability. Selected hydrogen atoms have been omitted for clarity, and the disorder in some of the isopropyl groups of the ligand is not shown.

unclear. It is likely that **5a** is thermodynamically preferred because it maximizes the opposing dipole interactions between the partially negatively charged chlorine atom in the Fe−Cl bond and the adjacent partially positively charged hydrogen atom in the N−H bond. Density functional theory (DFT) calculations on the structures of **5a** and **5a**^{Cis} indicate that **5a** is thermodynamically more favorable.[15] Similar behavior in solution was observed during the synthesis of **5b**.

The molecular structure of **5a** in the solid state is shown in Figure 4 and reveals a distorted octahedral geometry around the central iron atom, similar to those found for **1a** and **3a**. The data were of sufficient quality that the hydrogen atoms involved in the Fe−H and N−H bonds were located in the Fourier map and their positions refined without restraint. As suggested by ^{1}H NMR spectroscopy, the N−H bond is *trans* to the Fe−H bond. The Fe−H bond distance of 1.43(3) Å is comparable to that observed by Milstein and co-workers in {2,6-C_5H_3N-$(CH_2P^iPr_2)_2$}FeHBr(CO).[6a] The substitution of a chloride ligand on **1a** for a hydride ligand on **5a** results in significant C−O bond lengthening in the CO ligand, presumably because of the increased σ donation from the hydride ligand, which is consistent with the IR data. The C−O bond distance increases from 1.130(5) Å in **1a** to 1.168(2) Å in **5a**, while the Fe(1)−C(1) bond distance contracts from 1.736(4) Å in **1a** to 1.718(3) Å in **5a**. The Fe−Cl bond length increases from 2.3384(11) Å in **1a** to 2.4155(5) Å in **5a**, which is consistent with the increased *trans* influence of the hydride ligand.[18] The intramolecular Cl(1)−H(1N) distance is 2.58(3) Å. In the solid state, **5a** packs into dimers, with a pair of hydrogen bonds formed between the chloride ligand and the N−H proton on adjacent molecules (Figure 4b). The two hydrogen bonds have identical intermolecular Cl(1)−H(1N*) and Cl(1*)−H(1N) bond distances of 2.78(3) Å, which is significantly shorter than the combined van der Waals radii of hydrogen and chlorine.[19] The hydrogen bonds result in the formation of an essentially planar eight-membered ring and are consistent with the low N−H stretching frequency in the IR spectrum.

Preparation of Borohydride-Containing Complexes. The treatment of **1a** with 10 equiv of $NaBH_4$ in a 1:1 ACN/EtOH mixture results in the formation of the iron(II) borohydride complex (^{iPr}PNP)FeH(η^1-HBH_3)(CO) (**6a**), with no evidence for the formation of a dihydride species (eq 3). Complex **6a** is a rare example of a monomeric group 8 η^1-

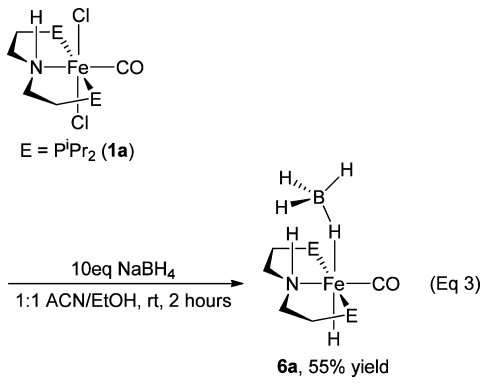

(Eq 3)

dx.doi.org/10.1021/ic402762v | *Inorg. Chem.* XXXX, XXX, XXX−XXX

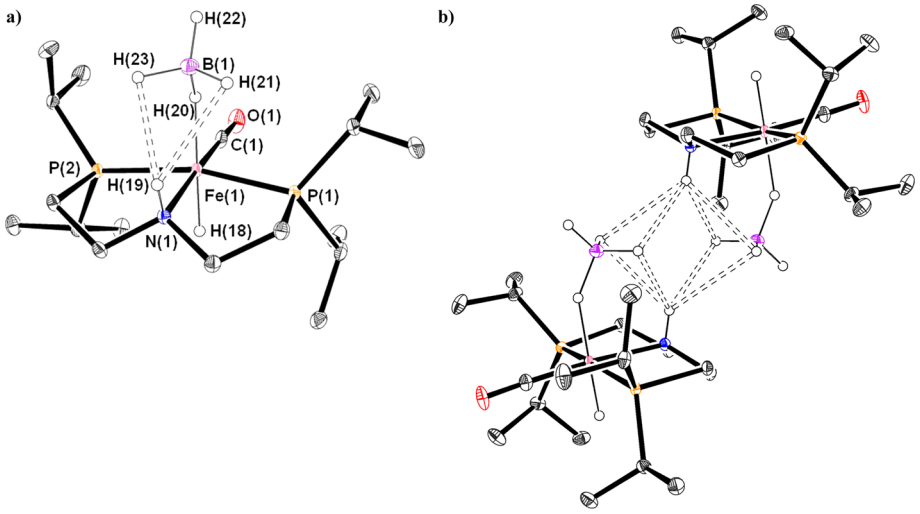

Figure 5. (a) ORTEP of **6a** at 50% probability. (b) Dimeric packing of **6a** at 50% probability. Selected hydrogen atoms have been omitted for clarity, and the disorder in the CO ligand is not shown.

HBH_3 complex.[6b,7,9a,b,d,f,g] The same product is obtained when excess $^{n}Bu_4NBH_4$ is used as the hydride and borohydride source, but in this case, longer reaction times (approximately 27 h) are required. In contrast, the treatment of the cyclohexyl-substituted complex **1b** with excess $NaBH_4$ or $^{n}Bu_4NBH_4$ resulted in the formation of a mixture of products, and it was not possible to isolate the analogous η^1-HBH_3 species to **6a**. The ^{1}H NMR spectrum of **6a** at room temperature contains a resonance corresponding to the proton of the terminal Fe−H at −19.5 ppm, similar to that of **5a**, and also a broad resonance centered at −2.5 ppm, which integrates to four protons and is assigned as the η^1-HBH_3 protons. When the ^{1}H NMR spectrum is recorded at −40 °C, the broad resonance at −2.5 ppm is decoalesced into two new signals at 0.9 and −14.8 ppm, respectively. The signal at −14.8 ppm integrates to one proton, while the signal at 0.9 ppm, which is partially obscured under resonances associated with the ^{iPr}PNP ligand, presumably integrates to three protons. These results are consistent with reduced η^1-HBH_3 fluxionality at low temperature, resulting in separate signals for the bridging Fe−H−B and terminal B−H protons, respectively. Indeed, 2D NOESY NMR experiments (−40 °C, mixing time = 400 ms) do exhibit exchange correlations between the protons associated with the resonance at 0.9 ppm and the proton corresponding to the resonance at −14.8 ppm, suggesting that interchange is still occurring at this temperature but at a slower rate.[15] Similar fluxional behavior in complexes containing an η^1-HBH_3 ligand has been previously observed by Baker and Field.[20] The NMR experiments also indicated an NOE correlation between the N−H resonances at 3.89 ppm and the terminal B−H protons at 0.9 ppm, establishing that the N−H bond is *cis* to the η^1-HBH_3 ligand and *trans* to the Fe−H bond.[15]The IR spectrum of **6a** is also consistent with an η^1-HBH_3 ligand. Well-defined stretches, which have been assigned based on previous literature precedent, are observed at 2352 (ν_{BH_3}), 2030 (ν_{Fe-H-B}), and 1069 (ν_{BH_3}) cm^{-1}.[20b] The CO stretching frequency at 1896 cm^{-1} is almost identical with the corresponding band in **5a**, indicating that the η^1-HBH_3 ligand donates an amount of electron density similar to the chloride ligand in **5a**. The N−H stretching frequency in **6a** is located at 3197 cm^{-1}, which is consistent with the participation of the coordinated amine in hydrogen bonding.

In a fashion analogous to the synthesis of **5a**, the reaction of **1a** with $NaBH_4$ results in an initial product mixture containing two species, one of which is **6a**. Upon standing at room temperature, the mixture converts entirely to **6a**. Again, we postulate that the other initial product is an isomer of **6a** in which the N−H bond is *trans* to the η^1-HBH_3 ligand and *cis* to the Fe−H bond (**6a**^{Cis}). In the room temperature ^{1}H NMR spectrum of the mixture, a clear signal at −22.0 ppm is assigned as the hydride of **6a**^{Cis}. At −40 °C, there are two different resonances in the ^{1}H NMR spectrum that are consistent with bridging Fe−H−B protons, supporting our hypothesis that both **6a** and **6a**^{Cis} are present. The ^{31}P{^{1}H} NMR chemical shift of **6a**^{Cis} (100.2 ppm) is also close to that of **6a** (99.1 ppm). In this case, we propose that dihydrogen bonding[12] between the N−H proton and the η^1-HBH_3 ligand (vide infra) results in **6a** being thermodynamically preferred over **6a**^{Cis}. DFT calculations also indicate that **6a** is the more stable isomer.[15]

The high-quality structure of **6a** from X-ray diffraction, which allowed for the location and refinement of the Fe−H, N−H, and B−H hydrogen atoms, is shown in Figure 5. To the best of our knowledge, there are only two previous examples of structurally characterized iron complexes containing an η^1-HBH_3 ligand.[6b,7] The molecular structure in the solid state confirms that the η^1-HBH_3 ligand and N−H bond are in a *cis* arrangement. Overall, the bond angles and lengths around the iron center in **6a** are very similar to those observed in **5a**. In particular, the C−O bond length in the CO ligand and the Fe−C bond length are almost identical in **5a** and **6a**, which provides further support that η^1-HBH_3 is electronically similar to the chloride ligand. The Fe(1)−H(20)−B(1) bond angle is bent [141.8(15)°] and is in the typical range for η^1-HBH_3 metal complexes.[6b,7] The Fe−B distance [2.745(2) Å] is also consistent with the two other iron complexes with η^1-HBH_3 ligands.[6b,7] The bridging Fe(1)−H(20) bond length [1.70(2) Å] is elongated compared to the terminal Fe−H bond length [1.45(2) Å]. Similarly, the bridging borohydride B(1)−H(20) bond distance [1.18(2) Å] is lengthened compared to the terminal B−H bonds [for example, the B(1)−H(22) bond distance is 1.09(2) Å].

dx.doi.org/10.1021/ic402762v | *Inorg. Chem.* XXXX, XXX, XXX−XXX

The structure of **6a** features a bifurcated intramolecular dihydrogen bond[12] between the η^1-HBH_3 ligand and the N−H bond of the PNP ligand. A close contact of 2.16(2) Å is observed within N(1)−H(19)···H(21)−B(1), and a second weaker contact of 2.43(3) Å is present within N(1)−H(19)···H(23)−B(1). Although 2.43(3) Å is slightly larger than the van der Waals radii (2.4 Å) of two hydrogen atoms,[19] considering the systematic underestimation of X−H bond distances inherent in X-ray crystallography,[21] we believe that this interaction is significant. Furthermore, Crabtree and co-workers report that in systems where a B−H···N−H dihydrogen bond is present, the B−H···H−N bond angle is bent to maximize the columbic interaction between the electropositive donor hydrogen atom and the electronegative acceptor boron atom.[12b−d] Indeed in **6a**, the angles of both proposed dihydrogen bonds are bent (the B(1)−H(21)−H(19) bond angle is 93(1)°, while the B(1)−H(23)−H(19) bond angle is 80(1)°), which provides further support for two dihydrogen bonds. Related examples of dihydrogen bonding have previously been observed in ruthenium complexes by Noyori and co-workers[9f] and Morris and co-workers[9g] and are believed to be important in the catalytic activity of these species.

Along with the bifurcated intramolecular dihydrogen bond, a bifurcated intermolecular dihydrogen bond is also present, which causes a dimeric packing of molecules in **6a** similar to that in **5a** (Figure 5b). However, unlike the planar bridging eight-membered ring formed by connecting the molecules in **5a**, a bridging distorted octahedron with hydrogen atoms occupying the six vertices is formed in **6a**. The intermolecular dihydrogen bond is formed between the B−H bonds of the η^1-HBH_3 ligand and the N−H bond of a neighboring molecule. The same B−H bonds that form the intramolecular dihydrogen bond also form the intermolecular dihydrogen bond, and similar geometrical parameters are observed in the intra- and intermolecular cases. In principle, dihydrogen bonding should result in increased B−H bond distances.[12b−d] However, in **6a**, the B−H bond lengths of the two bonds that are involved in dihydrogen bonds with the N−H moieties (B(1)−H(21) 1.12(2) and B(1)−H(23) 1.12(2) Å) are the same within error as the terminal B−H bond distance (B(1)−H(22) 1.09(2) Å).

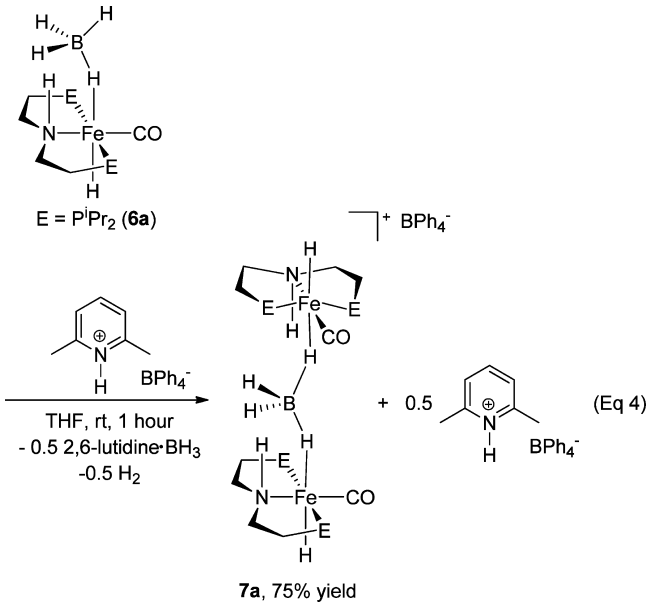

In an attempt to synthesize a dihydrogen complex, **6a** was treated with 1 equiv of 2,6-lutidinium tetraphenylborate in tetrahydrofuran (THF). Upon the addition of the acid, the solution rapidly changed from red to yellow, and the evolution of a gas was observed. The dimeric complex $[\{(^{i\text{Pr}}\text{PNP})\text{FeH}(\text{CO})\}_2(\mu_2,\eta^1{:}\eta^1\text{-}H_2BH_2)][BPh_4]$ (**7a**) was isolated in 75% yield, along with 0.5 equiv of 2,6-lutidinium tetraphenylborate, indicating that the reaction does not proceed further in the presence of excess acid (eq 4). When the reaction was repeated with 0.5 equiv of 2,6-lutidinium tetraphenylborate, **7a** was formed with full conversion of the starting material and H_2 evolution was observed by ^{1}H NMR spectroscopy. Compound **7a** is particularly noteworthy because it is the first dimeric group 8 species with a $\mu_2,\eta^1{:}\eta^1$-H_2BH_2 ligand and the only example of a transition-metal complex that contains a $\mu_2,\eta^1{:}\eta^1$-H_2BH_2 ligand, which does not also contain a bridging hydride and a metal−metal bond.[11] Therefore, the $\mu_2,\eta^1{:}\eta^1$-H_2BH_2 ligand in **7a** could be described as the first example of an "unsupported" bridging borohydride ligand, although because of dihydrogen bonding (vide infra), this is almost certainly not the case. In a fashion similar to that of the monomeric η^1-HBH_3 complex **6a**, **7a** exhibits fluxional behavior. In the ^{1}H NMR spectrum at room temperature, a single resonance is observed for the two terminal Fe−H protons at −21.9 ppm, while all of the protons associated with the $\mu_2,\eta^1{:}\eta^1$-H_2BH_2 ligand are equivalent and appear as a broad resonance at −5.7 ppm. When the spectrum is recorded at −80 °C, the broad peak at −5.7 ppm is no longer present, and two new resonances at 0.0 and −14.5 ppm, which integrate to two protons each, are observed. This is consistent with either no or slow exchange on the NMR time scale of the protons associated with $\mu_2,\eta^1{:}\eta^1$-H_2BH_2 at low temperature. It should be noted that complex **7a** is insoluble in most common NMR solvents and NMR data could only be recorded in CD_2Cl_2. In this solvent, **7a** is unstable at room temperature and decomposes in minutes. As a result, minor unidentified impurities are always present in the NMR spectrum. In the IR spectrum, the CO stretching frequency in **7a** (1901 cm^{-1}) is similar to that observed in **6a**, suggesting a similar electronic environment at the metal center. The molecular structure of **7a** from single-crystal X-ray diffraction is shown in Figure 6. It should be noted that the key hydrogen atoms associated with the Fe−H, B−H, and N−H bonds were all located and refined. The dimeric core of **7a** features a

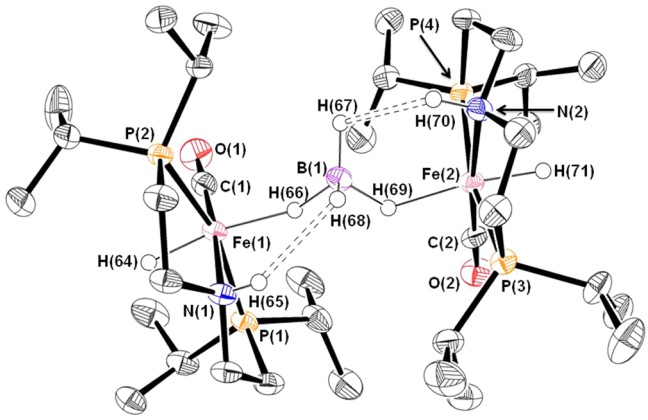

Figure 6. ORTEP of the cation of **7a** at 50% probability. Selected hydrogen atoms, the counterion, and the solvent of crystallization have been omitted for clarity.

dx.doi.org/10.1021/ic402762v | Inorg. Chem. XXXX, XXX, XXX−XXX

bridging borohydride ligand that coordinates to each iron center through a single B−H bond. Although the bond lengths and angles around the two iron centers are almost identical, the molecule does not possess any symmetry elements and the orientation of the ligands around the two iron centers differs by approximately 90°. The bond angles and distances around the iron and boron centers are consistent with those observed in the monomeric complex **6a** (Table 2). The two Fe−H(B) bridging bond distances in **7a** are 1.74(2) and 1.79(2) Å, while the two Fe−B bond lengths are 2.734(4) and 2.781(4) Å, consistent with the assigned $\mu_2,\eta^1:\eta^1$-H_2BH_2 coordination mode. The Fe(1)−Fe(2) bond distance is >5.2 Å, indicating that no metal−metal bond is present.

In a manner similar to that of **6a**, dihydrogen bonding is also featured in the core of **7a**. Unlike the bifurcated dihydrogen bonds seen in **6a**, each N−H bond in **7a** forms a single dihydrogen bond to the borohydride ligand, which creates two chelating six-membered rings. The N(1)−H(65)···H(68)−B(1) dihydrogen bond length is 2.06(4) Å, and the N(2)−H(70)···H(67)−B(1) bond length is 2.22(4) Å. As expected, the B−H···H−N angles of the atoms involved in both proposed dihydrogen bonds are bent [the B(1)−H(68)−H(65) bond angle is 112(2)°, and the B(1)−H(67)−H(70) bond angle is 95(2)°]. The B−H bonds that bridge to the iron atoms are longer than the B−H bonds that are involved in the dihydrogen interactions; B(1)−H(66) is 1.17(2) Å and B(1)−H(69) is 1.18(2) Å, whereas B(1)−H(67) is 1.11(2) Å and B(1)−H(68) is 1.11(2) Å. Overall, the dihydrogen-bonding interactions in **7a** presumably stabilize the $\mu_2,\eta^1:\eta^1$-H_2BH_2 ligand and make it more favorable for dimerization to occur. In fact, we suggest that these dihydrogen bonds play a role similar to that of the metal−metal bond and additional bridging hydride ligand observed in other examples of complexes with $\mu_2,\eta^1:\eta^1$-H_2BH_2 ligands and serve to "support" the $\mu_2,\eta^1:\eta^1$-H_2BH_2 ligand.[11]

CONCLUSIONS

The synthesis of a variety of iron complexes supported by ^{iPr}PNP and ^{Cy}PNP ligands is reported. A particularly interesting feature of these complexes is the ability of the proton on the N−H moiety of the PNP ligand to participate in both intra- and intermolecular hydrogen bonding and dihydrogen bonding with ligands that are coordinated to the iron center. For example, we have prepared a rare example of an iron complex with an η^1-HBH_3 ligand. In this species, two of the B−H bonds of the ligands participate in bifurcated dihydrogen bonds with the proton associated with the N−H group. Furthermore, we have prepared the first example of a dimeric iron complex with a $\mu_2,\eta^1:\eta^1$-H_2BH_2 ligand. In the previous examples of transition-metal complexes with a $\mu_2,\eta^1:\eta^1$-H_2BH_2 ligand, a metal−metal bond and another bridging ligand support the bridging borohydride ligand. In our case, there is no additional bridging ligand or Fe−Fe bond; however, we believe that dihydrogen bonds between protons of the N−H groups and the bridging borohydride ligands stabilize the complex. It is conceivable that this type of intramolecular dihydrogen bonding will influence the stoichiometric and catalytic reactivity of complexes with PNP ligands, and further studies toward this end are being conducted in our laboratories.

Table 2. Selected Bond Distances (Å) for the (^{iPr}PNP)Fe Complexes 6a and 7a

bond distance	6a	7a
Fe−B	2.745(2)	2.734(4), 2.781(4)
FeH−B	1.18(2)	1.17(2), 1.18(2)
BH···HN	1.12(2), 1.12(2)	1.11(2), 1.11(2)
B−H(t)	1.09(2)	
BH−HN	2.16(2), 2.43(3)	2.06(4), 2.22(4)

EXPERIMENTAL SECTION

General Methods. Experiments were performed under a dinitrogen or an argon atmosphere in an M-Braun drybox or using standard Schlenk techniques unless otherwise noted. Under standard glovebox conditions, purging was not performed between uses of pentane, diethyl ether, benzene, toluene, and THF; thus, when any of these solvents were used, traces of all of these solvents were in the atmosphere. Moisture- and air-sensitive liquids were transferred by a stainless steel cannula on a Schlenk line or in a drybox. The solvents for air- and moisture-sensitive reactions were dried by passage through a column of activated alumina followed by storage under dinitrogen or argon. All commercial chemicals were used as received except where noted. ^{iPr}PNP,[3d] ^{Cy}PNP,[22] ^{tBu}PNP[3u] and 2,6-lutidinium tetraphenylborate[23] were prepared using literature procedures. Anhydrous $FeCl_2$, $Fe(CO)_5$, HCl in Et_2O (2 M), $LiHBEt_3$ in THF (1 M), $NaBH_4$, $^nBu_4NBH_4$, and sodium tetraphenylborate were purchased from Aldrich and used as received. Deuterated solvents were obtained from Cambridge Isotope Laboratories. C_6D_6 was dried over sodium metal, CD_2Cl_2 was dried over calcium hydride, and acetone-d_6 was dried by stirring for 24 h over molecular sieves (3 Å) and for 24 h over activated B_2O_3. All deuterated solvents were distilled prior to use. NMR spectra were recorded on Bruker AMX-400, AMX-500, Avance 300, or Avance 500 spectrometers or on a Varian 300 MHz spectrometer at ambient probe temperatures unless noted. Chemical shifts are reported in ppm, with respect to a residual internal protio solvent for ^{1}H and ^{13}C NMR spectra and to an external standard for ^{31}P NMR spectra (85% H_3PO_4 at 0.0 ppm). IR spectra were measured using a diamond smart orbit ATR on a Nicolet 6700 FT-IR instrument or a Nujol mull between KBr plates on a Bruker Vertex 70 spectrometer. UV−vis spectra were measured using a Cary 50 spectrophotometer. Robertson Microlit Laboratories, Inc., and the analytical laboratory of the Institut für Anorganische Chemie (Universität Göttingen) performed the elemental analyses (inert atmosphere).

X-ray Crystallography. Crystal samples were mounted in MiTeGen polyimide loops with immersion oil. The diffraction experiments were carried out on a Rigaku SCXMini diffractometer with a Rigaku CCD detector using filtered Mo Kα radiation (λ = 0.71073 Å) for **1a**, a Bruker Nonius FR591 rotating-anode diffractometer with a Bruker Nonius Kappa CCD using Mo Kα radiation (λ = 0.71073 Å) for **2a** and **3a**, a STOE IPDS II diffractometer using Mo Kα radiation (λ = 0.71073 Å) for **4a**^{Trans}, a Rigaku MicroMax-007HF diffractometer coupled to a Saturn994 + CCD detector with Cu Kα radiation (λ = 1.54178 Å) for **5a**, or a Rigaku R-AXIS RAPID diffractometer coupled to a R-AXIS RAPID imaging plate detector with Mo Kα radiation (λ = 0.71073 Å) for **6a** and **7a**. For **1a**, **5a**, **6a**, and **7a**, the data frames were processed using Rigaku *CrystalClear*[24] and corrected for Lorentz and polarization effects. The structures were solved by direct methods[25] and expanded using Fourier techniques.[26] For **2a** and **3a**, the PLATON MULABS semiempirical absorption correction using multiple scanned reflections was applied. The structures were solved by direct methods, and the full-matrix least-squares refinement was carried out on F^2 using *SHELXTL NT 6.12*.[27] In all structures, non-hydrogen atoms were refined anisotropically and hydrogen atoms were treated as idealized contributions except where noted. Details of the crystal and refinement data for **1a**, **2a**, **3a**, **4a**^{Trans}, **5a**, **6a**, and **7a** are described in the Supporting Information.

Synthetic Procedures and Characterization Data for New Compounds. *(^{iPr}PNP)$FeCl_2$(CO) (**1a**). Route A.* A suspension of 10

dx.doi.org/10.1021/ic402762v | *Inorg. Chem.* XXXX, XXX, XXX−XXX

mg of anhydrous $FeCl_2$ (1 equiv, 0.080 mmol) and 25 mg of ^{iPr}PNP (1 equiv, 0.080 mmol) in 5 mL of THF was degassed using three freeze–pump–thaw cycles. CO (1 atm) was then introduced at room temperature using a dual-manifold Schlenk line. The resulting pale-purple suspension was stirred at room temperature for 2 h to give a deep-purple solution, the solvent was removed, and the solid was washed with 3 × 5 mL pentane to give **1a** as a purple solid. Crystals suitable for X-ray diffraction were grown from a saturated CH_2Cl_2 solution at −30 °C. Yield: 30 mg (0.065 mmol, 81%).

Route B. Complex **2a** (65 mg, 0.156 mmol) was dissolved in 20 mL of CH_2Cl_2 and stirred at room temperature for 12 h. The solution gradually changed from dark green to reddish brown. The solvent was evaporated to dryness and the residue washed with pentanes. The crude product was dissolved in THF and purified by column chromatography as a purple band from silanized silica (eluent: pentanes). The purple compound was dissolved in benzene and filtered, and the solvent was evaporated to obtain **1a** as a purple microcrystalline solid. Yield: 17 mg (0.037 mmol, 24%).

Anal. Found (calcd) for $C_{17}H_{37}Cl_2FeNOP_2$: C, 44.16 (44.37); H, 8.07 (8.10); N, 2.95 (3.04). ^{1}H NMR (400 MHz, CD_2Cl_2): 5.23 (br, 1H, N*H*), 3.62 (m, 2H, CH_2), 3.31 (dd, J = 25.0 Hz, $^3J_{HP}$ = 12.5 Hz, 2H, CH_2), 2.53 (m, 6H, CH_2, C*H*), 2.11 (m, 2H, C*H*), 1.45 (m, 12H, CH_3), 1.38 (m, 12H, CH_3). ^{13}C{^{1}H} NMR (125 MHz, CD_2Cl_2): 50.1 (vt, J_{CP} = 4.5 Hz), 26.8 (vt, J_{CP} = 6.7 Hz), 23.8 (vt, J_{CP} = 10.7 Hz), 21.9 (vt, J_{CP} = 9.2 Hz), 20.2, 19.9, 19.0, 18.8; CO resonance was not detected. ^{31}P{^{1}H} NMR (162 MHz, CD_2Cl_2): 67.9. IR (cm^{-1}): 3204 (ν_{NH}), 1926 (ν_{CO}). UV–vis [THF; λ_{max}, nm (ε, L mol^{-1} cm^{-1})]: 226 (12929), 261 (10070), 322 (27724), 560 (117).

*(^{Cy}PNP)FeCl$_2$(CO) (**1b**).* A suspension of 7 mg of anhydrous $FeCl_2$ (1 equiv, 0.053 mmol) and 25 mg of ^{Cy}PNP (1 equiv, 0.053 mmol) in 5 mL of THF was degassed using three freeze–pump–thaw cycles. CO (1 atm) was then introduced at room temperature using a dual-manifold Schlenk line. The resulting pale-purple suspension was stirred at 50 °C for 4 h to give a deep-purple solution, the solvent was removed, and the solid was washed with 3 × 5 mL pentane to give **3b** as a purple solid. Yield: 23 mg (0.037 mmol, 70%).

Anal. Found (calcd) for $C_{29}H_{53}Cl_2FeNOP_2$: C, 56.95 (56.14); H, 8.74 (8.61); N, 2.16 (2.26). ^{1}H NMR (400 MHz, CD_2Cl_2): 5.21 (br, 1H, N*H*), 3.56 (m, 2H, CH_2), 3.27 (m, 2H, CH_2), 2.47 (br, 2H), 2.24 (br, 5H) 2.09 (t, J = 13.3 Hz, 4H), 1.95–1.62 (m, 22H), 1.26 (t, J = 10.4 Hz, 6H), 1.13 (t, J = 9.7 Hz, 4H). ^{13}C{^{1}H} NMR (C_6D_6, 75 MHz): 49.4 (vt, J_{CP} = 5.4 Hz), 34.5 (vt, J_{CP} = 10.1 Hz), 32.7 (vt, J_{CP} = 8.5 Hz), 30.6, 29.7, 29.1 (d, J_{CP} = 18.4 Hz), 28.79 (m), 27.2 (m), 26.7 (d, J_{CP} = 4.6 Hz), 24.6 (vt, J_{CP} = 6.2 Hz); CO resonance was not detected. ^{31}P{^{1}H} NMR (162 MHz, CD_2Cl_2): 58.9. IR (cm^{-1}): 3188 (ν_{NH}), 1944 (ν_{CO}). UV–vis [THF; λ_{max}, nm (ε, L mol^{-1} cm^{-1})]: 212 (16891), 263 (10123), 325 (3246), 475 (177).

*(^{iPr}PNP)Fe(CO)$_2$ (**2a**).* A total of 100 mg of Fe(CO)$_5$ (1 equiv, 0.510 mmol) was dissolved in 5 mL of acetone, and 156 mg of ^{iPr}PNP (1 equiv, 0.510 mmol) in 5 mL of acetone was added. The pale-yellow solution was stirred and irradiated with a 150 W xenon short arc lamp for 150 min at room temperature. The deep-red solution was evaporated to dryness and the residue washed with 4 × 8 mL pentanes. The remaining red product was lyophilized from a benzene solution to obtain **2a** as an orange powder. Crystals suitable for X-ray diffraction were grown by diffusion of pentanes into a saturated THF solution at room temperature. Yield: 120 mg (0.288 mmol, 56%).

Anal. Found (calcd) for $C_{18}H_{37}FeNO_2P_2$: C, 51.79 (51.81); H, 8.85 (8.94); N, 3.36 (3.36). ^{1}H NMR (500 MHz, acetone-d_6): 3.18 (m, 2H, CH_2), 2.35 (m, 2H, C*H*), 2.23 (m, 2H, C*H*), 1.98 (m, 4H, CH_2), 1.68 (m, 2H, CH_2), 1.31 (m, 12H, CH_3), 1.21 (m, 12H, CH_3); the N*H* proton was not detected presumably because of H/D exchange with the solvent. ^{13}C{^{1}H} NMR (125 MHz, acetone-d_6): 226.2 (t, J_{CP} = 34.4 Hz), 222.4 (t, J_{CP} = 19.5 Hz), 54.7 (vt, J_{CP} = 5.3 Hz), 27.9 (vt, J_{CP} = 10.5 Hz), 26.4 (vt, J_{CP} = 11.8 Hz), 25.0 (vt, J_{CP} = 5.6 Hz), 19.2, 18.2, 17.0. ^{31}P{^{1}H} NMR (200 MHz, acetone-d_6): 109.8. IR (Nujol, cm^{-1}): 3263 (ν_{NH}), 1838 (ν_{CO}), 1767 (ν_{CO}).

*cis- and trans-[(^{iPr}PNP)FeH(CO)$_2$]Cl (**4a**).* A total of 50 mg of **2a** (1 equiv, 0.120 mmol) was dissolved in 8 mL of THF, and a solution of 6.56 mg of HCl (1.5 equiv, 0.180 mmol) in Et_2O (2 M) was added. A color change to pale yellow and precipitation of a colorless solid were observed. The solution was stirred for 10 min at room temperature, the solvent was evaporated under vacuum, and the beige residue was lyophilized from benzene to give **4a** as a beige solid. Yield: 50 mg (0.11 mmol, 93%). The spectroscopic characterization is in agreement with a mixture of two isomers as described in the text (A (*trans*) and B (*cis*)) in a 3:1 ratio with the *trans* and *cis* arrangements of the N–H and Fe–H moieties.

Anal. Found (calcd) for $C_{18}H_{38}ClFeNO_2P_2$: C, 47.30 (47.65); H, 8.56 (8.44); N, 2.99 (3.09). ^{1}H NMR (500 MHz, CD_2Cl_2): 6.48 (s br, 1H, N*H*^{A}), 5.91 (s br, 1H, N*H*^{B}), 2.71 (br, 2H, CH_2^A), 2.41 (m, 4H, C*H*^{A}), 2.05 (br, 2H, CH_2^A), 1.93 (br, 2H, CH_2^A), 1.82 (br, 2H, CH_2^A), 1.46 (dd, J = 7.2 Hz, $^3J_{HP}$ = 15.7 Hz, 6H, CH_3^A), 1.38 (dd, J = 6.9 Hz, $^3J_{HP}$ = 13.8 Hz, 6H, CH_3^A), 1.33 (m, 12H, CH_3^B), 1.23 (m, 12H, CH_3^A), −7.38 (t, $^2J_{HP}$ = 48.8 Hz, 1H, Fe*H*^{B}), −8.22 (t, $^2J_{HP}$ = 44.8 Hz, 1H, Fe*H*^{A}); not all resonances for isomer B (*cis*) were identified. ^{13}C{^{1}H} NMR (75 MHz, CD_2Cl_2): 54.7 (vt, J_{CP} = 3.5 Hz, NC$^AH_2$), 32.2 (vt, J_{CP} = 11.9 Hz, C^{A}H), 30.2 (vt, J_{CP} = 10.5 Hz, C$^AH_2$), 28.4 (vt, J_{CP} = 10.1 Hz, C$^BH_2$), 26.5 (vt, J_{CP} = 14.0 Hz, C^{A}H), 21.1 (s, C$^BH_3$), 20.5 (s, C$^BH_3$), 20.2 (s, C$^AH_3$), 20.1 (s, C$^AH_3$), 19.2 (s, C$^AH_3$), 19.1 (s, C$^BH_3$), 18.9 (s, C$^AH_3$), 18.7 (s, C$^BH_3$); CO resonances were not detected. ^{31}P{^{1}H} NMR (120 MHz, CD_2Cl_2): 102.1 (s, P^B), 99.5 (s, P^A). IR (Nujol, cm^{-1}): 1998 (ν_{CO}), 1987 (ν_{CO}), 1943 (ν_{CO}), 1932 (ν_{CO}).

*(^{iPr}PNP)FeHCl(CO) (**5a**). Route A.* To a solution of 200 mg of **1a** (1 equiv, 0.434 mmol) in 1 mL of ACN was added 110 mg of $^nBu_4NBH_4$ (1 equiv, 0.428 mmol) at room temperature. The solution changed from purple to orange upon the addition of $^nBu_4NBH_4$. The reaction mixture was stirred for 48 h at ambient temperature, after which time the volatiles were removed in vacuo. The residue was extracted with 3 × 5 mL of 2:1 Et_2O/benzene and then cooled to −30 °C. Compound **5a** was isolated as orange crystals. Crystals suitable for X-ray diffraction were grown from a saturated Et_2O solution at −30 °C. Yield: 70 mg (0.16 mmol, 38%).

Route B. Compound **1a** (100 mg, 0.217 mmol) was dissolved in 12 mL of THF and cooled to −50 °C. A cold solution (−50 °C) of $LiHBEt_3$ (0.240 mmol) in THF (1 M) was slowly added, and the solution was allowed to warm to room temperature over 150 min. The reaction mixture slowly changed from dark red to reddish yellow. After evaporation of the solvent, the residue was washed with 6 mL of pentanes, extracted with Et_2O/benzene (3:1), and crystallized at −38 °C. Compound **5a** was isolated as orange crystals. Yield: 45 mg (0.11 mmol, 51%).

Anal. Found (calcd) for $C_{17}H_{38}ClFeNOP_2$: C, 47.69 (47.96); H, 9.01 (9.00) N, 3.24 (3.29). ^{1}H NMR (500 MHz, CD_2Cl_2): 3.69 (br, 1H, N*H*), 2.93 (m, 2H, CH_2), 2.76 (m, 2H, CH_2), 2.02 (m, 2H, C*H*), 1.70 (m, 10H, CH_3 and CH_2), 1.55 (m, 2H, C*H*), 1.24 (m, 6H, CH_3), 1.18 (m, 6H, CH_3), 0.92 (m, 6H, CH_3), −19.1 (t, $^2J_{HP}$ = 52.7 Hz, 1H, Fe*H*). ^{13}C{^{1}H} NMR (125 MHz, CD_2Cl_2): 53.6 (vt, J_{CP} = 5.7 Hz), 29.3 (vt, J_{CP} = 6.6 Hz), 27.0 (vt, J_{CP} = 9.1 Hz), 25.0 (vt, J_{CP} = 12.0 Hz), 20.7, 20.6 (vt, J_{CP} = 2.4 Hz), 19.1, 18.0 (vt, J_{CP} = 2.1 Hz); CO resonance was not detected. ^{31}P{^{1}H} NMR (162 MHz, CD_2Cl_2): 95.4. IR (cm^{-1}): 3183 (ν_{NH}), 1895 (ν_{CO}), 1849. UV–vis [THF; λ_{max}, nm (ε, L mol^{-1} cm^{-1})]: 223 (12890), 336 (472), 438 (475).

*(^{Cy}PNP)FeHCl(CO) (**5b**).* To a solution of 87 mg of **1b** (1 equiv, 0.14 mmol) in 6 mL of ACN was added 36 mg of $^nBu_4NBH_4$ (1 equiv, 0.14 mmol) at room temperature. The solution changed from purple to yellow upon the addition of $^nBu_4NBH_4$. The reaction mixture was stirred for 48 h at ambient temperature, after which time the volatiles were removed in vacuo. The residue was extracted with 3 × 5 mL of 3:1 Et_2O/benzene and then cooled to −30 °C. The precipitate was isolated and washed with pentane to yield **1b** as a yellow-orange powder. Yield: 66 mg (0.11 mmol, 80%).

Anal. Found (calcd) for $C_{17}H_{38}ClFeNOP_2$: C, 59.52 (59.44), H, 9.34 (9.29); N, 2.44 (2.39). ^{1}H NMR (300 MHz, C_6D_6): 3.74 (t, $^3J_{HP}$ = 13.5 Hz, 1H, N*H*), 3.10 (m, 2H, CH_2), 2.71 (m, 4H, CH_2), 2.18 (m, 2H, CH_2), 1.66 (m, 30H, Cy), 1.20 (m, 14H, Cy), −23.64 (t, $^2J_{HP}$ = 51.9 Hz, 1H, Fe*H*). ^{13}C{^{1}H} NMR (75 MHz, C_6D_6): 53.8 (vt, J_{CP} =

dx.doi.org/10.1021/ic402762v | *Inorg. Chem.* XXXX, XXX, XXX–XXX

5.6 Hz), 37.9 (vt, J_{CP} = 9.0 Hz), 36.4 (vt, J_{CP} = 11.1 Hz), 31.1, 30.7, 28.8 (vt, J_{CP} = 3.7 Hz), 27.4 (vt, J_{CP} = 5.3 Hz), 27.2, 26.9, 26.6; CO resonance was not detected. $^{31}P\{^1H\}$ NMR (162 MHz, C_6D_6): 88.6. IR (cm^{-1}): 3134 (ν_{NH}), 1895 (ν_{CO}), 1892. UV−vis [THF; λ_{max}, nm (ε, L mol^{-1} cm^{-1})]: 227 (10244), 329 (725), 447 (395).

*(^{iPr}PNP)FeH(η^1-HBH$_3$)(CO) (**6a**).* To a suspension of 846 mg of **1a** (1 equiv, 1.83 mmol) and 690 mg of $NaBH_4$ (10 equiv, 18.4 mmol) in 5 mL of ACN was added 5 mL of EtOH at room temperature. The solution changed from purple to yellow upon the addition of EtOH, and gas evolution was observed. The reaction mixture was stirred for 2 h at ambient temperature, after which time the volatiles were removed in vacuo. The solid was extracted with 5 × 10 mL of toluene, and the volatiles were removed under reduced pressure. A total of 5 mL of benzene was introduced, and the mixture was stirred for 48 h. The benzene was removed under vacuum, providing **6a** as a yellow powder. Crystals suitable for X-ray diffraction were grown from a saturated pentane/Et_2O solution at −30 °C. Yield: 360 mg (0.888 mmol, 55%).

Anal. Found (calcd) for $C_{17}H_{42}BFeNOP_2$: C, 50.28 (50.40); H, 10.28 (10.45); N, 3.35 (3.46). ^1H NMR (500 MHz, C_6D_6): 3.89 (br, 1H, N*H*), 2.79 (m, 2H, CH_2), 2.45 (m, 2H, CH_2), 1.99 (m, 2H, C*H*), 1.71 (m, 2H, CH_2), 1.61−1.43 (m, 10H, C*H*, CH_2, and CH_3), 1.20 (m, 6H, CH_3), 1.11 (m, 6H, CH_3), 0.90 (m, 6H, CH_3), −2.58 (br, 4H, BH_4), −19.52 (t, $^2J_{HP}$ = 50.7 Hz, 1H, Fe*H*). $^{13}C\{^1H\}$ NMR (125 MHz, C_6D_6): 54.0 (vt, J_{CP} = 5.5 Hz), 29.5 (vt, J_{CP} = 9.6 Hz), 28.9 (vt, J_{CP} = 7.1 Hz), 25.6 (vt, J_{CP} = 12.5 Hz), 20.7, 20.4, 19.0, 18.4; CO resonance was not detected. $^{31}P\{^1H\}$ NMR (162 MHz, C_6D_6): 99.1. IR (cm^{-1}): 3197 (ν_{NH}), 2352 (ν_{BH_3}), 2030 (ν_{Fe-H-B}), 1896 (ν_{CO}), 1831, 1068 (ν_{BH_3}). UV−vis [THF; λ_{max}, nm (ε, L mol^{-1} cm^{-1})]: 210 (11728), 280 (2581), 400 (302), 468 (131).

*[{(^{iPr}PNP)FeH(CO)}$_2$(μ_2,η^1:η^1-H$_2$BH$_2$)][BPh$_4$] (**7a**).* To 22 mg of **6a** (1 equiv, 5.4 μmol) and 24 mg of 2,6-lutidinium tetraphenylborate (1 equiv, 5.6 μmol) was added 0.5 mL of THF at room temperature. The reaction mixture was stirred for 1 h, after which time 2 mL of benzene was added to precipitate the remaining 2,6-lutidinium tetraphenylborate. The reaction mixture was filtered and the filtrate concentrated under vacuum to give **7a** as a yellow powder. Crystals suitable for X-ray diffraction were grown from a saturated THF solution at −30 °C. Yield: 6.0 mg (4.1 μmol, 75%).

Anal. Found (calcd): C, 62.12 (62.50); H, 8.78 (9.04); N, 2.39 (2.51). ^1H NMR (500 MHz, CD_2Cl_2): 7.38 (br, 8H, BPh_4), 7.02 (br, 8H, BPh_4), 6.85 (br, 4H, BPh_4), 3.85 (br, 4H, CH_2), 3.17 (br, 4H, CH_2), 2.74 (br, 2H, N*H*), 2.38 (br, 4H, CH_2), 2.28 (br, 4H, C*H*), 2.04 (br, 4H, CH_2), 1.90 (br, 6H, CH_3), 1.58 (br, 4H, C*H*), 1.49 (br, 6H, CH_3), 1.32 (br, 12H, CH_3), 1.21 (br, 12H, CH_3), 1.11 (br, 12H, CH_3), −6.90 (br, 4H, BH_4), −22.0 (t, $^2J_{HP}$ = 54.5 Hz, 2H, Fe*H*). $^{31}P\{^1H\}$ NMR (162 MHz, CD_2Cl_2): 93.9. IR (cm^{-1}): 3219 (ν_{NH}), 2004 (ν_{Fe-H-B}), 1901 (ν_{CO}), 1062 (ν_{BH_4}). UV−vis [THF; λ_{max}, nm (ε, L mol^{-1} cm^{-1})]: 210 (85880), 277 (4101), 446 (641). No ^{13}C NMR data were collected on this compound because of its low solubility in all common solvents, except for CD_2Cl_2, in which it was unstable.

■ ASSOCIATED CONTENT

Ⓢ Supporting Information

Selected ^1H, $^{31}P\{^1H\}$, and 2D NMR spectra, X-ray crystallographic information in CIF format for **1a**, **2a**, **3a**, **4a**^{Trans}, **5a**, **6a**, and **7a**, and details of DFT calculations. This material is available free of charge via the Internet at http://pubs.acs.org.

■ AUTHOR INFORMATION

Corresponding Authors

*E-mail: nilay.hazari@yale.edu.

*E-mail:sven.schneider@chemie.uni-goettingen.de.

Author Contributions

‡These authors made equal contributions.

Notes

The authors declare no competing financial interest.

■ ACKNOWLEDGMENTS

We thank Professor Gary Brudvig for access to his UV−vis spectrometer and Professor Siegfried Schindler and Jonathan Becker for access to the Bruker Nonius Kappa CCD diffractomer at Justus-Liebig-Universität Giessen. We gratefully acknowledge support from the National Science Foundation through the Centre for Chemical Innovation "CO_2 as a Sustainable Feedstock for Chemical Commodities" (Grant CHE-1240020) and from the Deutsche Forschungsgemeinschaft (Grant SCHN 950/4-1). This work was supported in part by the facilities and staff of the Yale University Faculty of Arts and Sciences High Performance Computing Center and by the National Science Foundation under Grant CNS 08-21132, which partially funded acquisition of the facilities.

■ REFERENCES

(1) Moulton, C. J.; Shaw, B. L. *J. Chem. Soc., Dalton Trans.* **1976**, *11*, 1020.

(2) (a) Albrecht, M.; van Koten, G. *Angew. Chem., Int. Ed.* **2001**, *40*, 3750. (b) van der Boom, M. E.; Milstein, D. *Chem. Rev.* **2003**, *103*, 1759. (c) Leis, W.; Mayer, H. A.; Kaska, W. C. *Coord. Chem. Rev.* **2008**, *252*, 1787. (d) Benito-Garagorri, D.; Kirchner, K. *Acc. Chem. Res.* **2008**, *41*, 201. (e) Selander, N.; Szabó, K. J. *Chem. Rev.* **2010**, *111*, 2048. (f) Albrecht, M.; Lindner, M. M. *Dalton Trans.* **2011**, *40*, 8733.

(3) (a) Bianchini, C.; Innocenti, P.; Peruzzini, M.; Romerosa, A.; Zanobini, F. *Organometallics* **1996**, *15*, 272. (b) Danopoulos, A. A.; Edwards, P. G. *Polyhedron* **1989**, *8*, 1339. (c) Danopoulos, A. A.; Edwards, P. G.; Parry, J. S.; Wills, A. R. *Polyhedron* **1989**, *8*, 1767. (d) Danopoulos, A. A.; Wills, A. R.; Edwards, P. G. *Polyhedron* **1990**, *9*, 2413. (e) Clarke, Z. E.; Maragh, P. T.; Dasgupta, T. P.; Gusev, D. G.; Lough, A. J.; Abdur-Rashid, K. *Organometallics* **2006**, *25*, 4113. (f) Choualeb, A.; Lough, A. J.; Gusev, D. G. *Organometallics* **2007**, *26*, 3509. (g) Amoroso, D.; Graham, T. W.; Guo, R.; Tsang, C.-W.; Abdur-Rashid, K. *Aldrichimica Acta* **2008**, *41*, 15. (h) Chen, X.; Jia, W.; Guo, R.; Graham, T. W.; Gullons, M. A.; Abdur-Rashid, K. *Dalton Trans.* **2009**, 1407. (i) Bertoli, M.; Choualeb, A.; Lough, A. J.; Moore, B.; Spasyuk, D.; Gusev, D. G. *Organometallics* **2011**, *30*, 3479. (j) Rozenel, S. S.; Kerr, J. B.; Arnold, J. *Dalton Trans.* **2011**, *40*, 10397. (k) Rozenel, S. S.; Arnold, J. *Inorg. Chem.* **2012**, *51*, 9730. (l) Rozenel, S. S.; Padilla, R.; Arnold, J. *Inorg. Chem.* **2013**, *52*, 11544. (m) McGuinness, D. S.; Wasserscheid, P.; Keim, W.; Hu, C.; Englert, U.; Dixon, J. T.; Grove, C. *Chem. Commun.* **2003**, 334. (n) McGuinness, D. S.; Wasserscheid, P.; Morgan, D. H.; Dixon, J. T. *Organometallics* **2005**, *24*, 552. (o) Schmeier, T. J.; Dobereiner, G. E.; Crabtree, R. H.; Hazari, N. *J. Am. Chem. Soc.* **2011**, *133*, 9274. (p) Friedrich, A.; Drees, M.; auf der Günne, J. S.; Schneider, S. *J. Am. Chem. Soc.* **2009**, *131*, 17552. (q) Friedrich, A.; Drees, M.; Schneider, S. *Chem.—Eur. J.* **2009**, *15*, 10339. (r) Friedrich, A.; Ghosh, R.; Kolb, R.; Herdtweck, E.; Schneider, S. *Organometallics* **2009**, *28*, 708. (s) Käss, M.; Friedrich, A.; Drees, M.; Schneider, S. *Angew. Chem., Int. Ed.* **2009**, *48*, 905. (t) Marziale, A. N.; Herdtweck, E.; Eppinger, J.; Schneider, S. *Inorg. Chem.* **2009**, *48*, 3699. (u) Meiners, J.; Friedrich, A.; Herdtweck, E.; Schneider, S. *Organometallics* **2009**, *28*, 6331. (v) Askevold, B.; Khusniyarov, M. M.; Herdtweck, E.; Meyer, K.; Schneider, S. *Angew. Chem., Int. Ed.* **2010**, *49*, 7566. (w) Friedrich, A.; Drees, M.; Käss, M.; Herdtweck, E.; Schneider, S. *Inorg. Chem.* **2010**, *49*, 5482. (x) Askevold, B.; Nieto, J.; Tussupbayev, S.; Diefenbach, M.; Herdtweck, E.; Holthausen, M.; Schneider, S. *Nat. Chem.* **2011**, *3*, 532. (y) Meiners, J.; Scheibel, M. G.; Lemee-Cailleau, M.-H.; Mason, S. A.; Boeddinghaus, M. B.; Faessler, T. F.; Herdtweck, E.; Khusniyarov, M. M.; Schneider, S. *Angew. Chem., Int. Ed.* **2011**, *50*, 8184. (z) Scheibel, M. G.; Askevold, B.; Heinemann, F. W.; Reijerse, E. J.; de Bruin, B.; Schneider, S. *Nat. Chem.* **2012**, *4*, 552. (aa) Schneider, S.; Meiners, J.; Askevold, B. *Eur. J. Inorg. Chem.* **2012**, *2012*, 412. (ab) Marziale, A. N.; Friedrich, A.; Klopsch, I.; Drees, M.; Celinski, V. R.; auf der Günne, J. S.; Schneider, S. *J. Am. Chem. Soc.* **2013**, *135*, 13342. (ac) Scheibel, M. G.; Wu, Y.; Stückl, A. C.; Krause, L.; Carl, E.; Stalke, D.; de Bruin, B.;

Schneider, S. *J. Am. Chem. Soc.* **2013**, *135*, 17719. (ad) Nielsen, M.; Alberico, E.; Baumann, W.; Drexler, H.-J.; Junge, H.; Gladiali, S.; Beller, M. *Nature* **2013**, *495*, 85. (ae) Zhang, G.; Scott, B. L.; Hanson, S. K. *Angew. Chem., Int. Ed.* **2012**, *51*, 11907. (af) Zhang, G.; Hanson, S. K. *Org. Lett.* **2013**, *15*, 650. (ag) Zhang, G.; Hanson, S. K. *Chem. Commun.* **2013**, *49*, 10151. (ah) Zhang, G.; Vasudevan, K. V.; Scott, B. L.; Hanson, S. K. *J. Am. Chem. Soc.* **2013**, *135*, 8668.

(4) While this work was being revised, Beller and co-workers reported the synthesis of three iron complexes supported by the ^{Pr}PNP ligand in: Alberico, E.; Sponholz, P.; Cordes, C.; Nielsen, M.; Drexler, H.-J.; Baumann, W.; Junge, H.; Beller, M. *Angew. Chem., Int. Ed.* **2013**, *52*, 14162.

(5) (a) Sui-Seng, C.; Freutel, F.; Lough, A. J.; Morris, R. H. *Angew. Chem., Int. Ed.* **2008**, *47*, 940. (b) Mikhailine, A. A.; Kim, E.; Dingels, C.; Lough, A. J.; Morris, R. H. *Inorg. Chem.* **2008**, *47*, 6587. (c) Mikhailine, A.; Lough, A. J.; Morris, R. H. *J. Am. Chem. Soc.* **2009**, *131*, 1394. (d) Sui-Seng, C.; Haque, F. N.; Hadzovic, A.; Putz, A.-M.; Reuss, V.; Meyer, N.; Lough, A. J.; Zimmer-De Iuliis, M.; Morris, R. H. *Inorg. Chem.* **2009**, *48*, 735. (e) Meyer, N.; Lough, A. J.; Morris, R. H. *Chem.—Eur. J.* **2009**, *15*, 5605. (f) Lagaditis, P. O.; Lough, A. J.; Morris, R. H. *Inorg. Chem.* **2010**, *49*, 10057. (g) Lagaditis, P. O.; Mikhailine, A. A.; Lough, A. J.; Morris, R. H. *Inorg. Chem.* **2010**, *49*, 1094. (h) Mikhailine, A. A.; Morris, R. H. *Inorg. Chem.* **2010**, *49*, 11039. (i) Lagaditis, P. O.; Lough, A. J.; Morris, R. H. *J. Am. Chem. Soc.* **2011**, *133*, 9662. (j) Sues, P. E.; Lough, A. J.; Morris, R. H. *Organometallics* **2011**, *30*, 4418. (k) Sonnenberg, J. F.; Coombs, N.; Dube, P. A.; Morris, R. H. *J. Am. Chem. Soc.* **2012**, *134*, 5893. (l) Mikhailine, A. A.; Maishan, M. I.; Lough, A. J.; Morris, R. H. *J. Am. Chem. Soc.* **2012**, *134*, 12266. (m) Mikhailine, A. A.; Maishan, M. I.; Morris, R. H. *Org. Lett.* **2012**, *14*, 4638. (n) Prokopchuk, D. E.; Morris, R. H. *Organometallics* **2012**, *31*, 7375. (o) Prokopchuk, D. E.; Sonnenberg, J. F.; Meyer, N.; Zimmer-De Iuliis, M.; Lough, A. J.; Morris, R. H. *Organometallics* **2012**, *31*, 3056. (p) Sonnenberg, J. F.; Morris, R. H. *ACS Catal.* **2013**, *3*, 1092.

(6) (a) Langer, R.; Leitus, G.; Ben-David, Y.; Milstein, D. *Angew. Chem., Int. Ed.* **2011**, *50*, 2120. (b) Langer, R.; Iron, M. A.; Konstantinovski, L.; Diskin-Posner, Y.; Leitus, G.; Ben-David, Y.; Milstein, D. *Chem.—Eur. J.* **2012**, *18*, 7196.

(7) Bau, R.; Yuan, H. S. H.; Baker, M. V.; Field, L. D. *Inorg. Chim. Acta* **1986**, *114*, L27.

(8) (a) Marks, T. J.; Kolb, J. R. *Chem. Rev.* **1977**, *77*, 263. (b) Xu, Z.; Lin, Z. *Coord. Chem. Rev.* **1996**, *156*, 139. (c) Besora, M.; Lledós, A. *Struct. Bonding (Berlin)* **2008**, *130*, 149.

(9) (a) Bianchini, C.; Perez, P. J.; Peruzzini, M.; Zanobini, F.; Vacca, A. *Inorg. Chem.* **1991**, *30*, 279. (b) Yoshida, T.; Adachi, T.; Ueda, T.; Akao, H.; Tanaka, T.; Goto, F. *Inorg. Chim. Acta* **1995**, *231*, 95. (c) Liang, F.; Jacobsen, H.; Schmalle, H. W.; Fox, T.; Berke, H. *Organometallics* **2000**, *19*, 1950. (d) Gusev, D. G.; Dolgushin, F. M.; Antipin, M. Y. *Organometallics* **2000**, *19*, 3429. (e) Höck, J.; Jacobsen, H.; Schmalle, H. W.; Artus, G. R. J.; Fox, T.; Amor, J. I.; Bäth, F.; Berke, H. *Organometallics* **2001**, *20*, 1533. (f) Ohkuma, T.; Koizumi, M.; Muñiz, K.; Hilt, G.; Kabuto, C.; Noyori, R. *J. Am. Chem. Soc.* **2002**, *124*, 6508. (g) Guo, R.; Morris, R. H.; Song, D. *J. Am. Chem. Soc.* **2004**, *127*, 516.

(10) (a) Holah, D. G.; Hughes, A. N.; Maciaszek, S.; Magnuson, V. R. *J. Chem. Soc., Chem. Commun.* **1983**, 1308. (b) Green, B. E.; Kennard, C. H. L.; Smith, G.; James, B. D.; Healy, P. C.; White, A. H. *Inorg. Chim. Acta* **1984**, *81*, 147. (c) Rhodes, L. F.; Venanzi, L. M.; Sorato, C.; Albinati, A. *Inorg. Chem.* **1986**, *25*, 3335. (d) Golub, I. E.; Filippov, O. A.; Gutsul, E. I.; Belkova, N. V.; Epstein, L. M.; Rossin, A.; Peruzzini, M.; Shubina, E. S. *Inorg. Chem.* **2012**, *51*, 6486.

(11) (a) Gilbert, T. M.; Hollander, F. J.; Bergman, R. G. *J. Am. Chem. Soc.* **1985**, *107*, 3508. (b) Carreno, R.; Riera, V.; Ruiz, M. A.; Bois, C.; Jeannin, Y. *Organometallics* **1993**, *12*, 1946.

(12) (a) Dihydrogen bonding is the interaction of a proton donor (N−H and O−H) with a metal hydride acceptor (most commonly B−H or M−H). This bonding can occur in an intra- or intermolecular fashion. (b) Lee, J. C.; Peris, E.; Rheingold, A. L.; Crabtree, R. H. *J. Am. Chem. Soc.* **1994**, *116*, 11014. (c) Crabtree, R. H.; Siegbahn, P. E. M.; Eisenstein, O.; Rheingold, A. L.; Koetzle, T. F. *Acc. Chem. Res.* **1996**, *29*, 348. (d) Klooster, W. T.; Koetzle, T. F.; Siegbahn, P. E. M.; Richardson, T. B.; Crabtree, R. H. *J. Am. Chem. Soc.* **1999**, *121*, 6337.

(13) Benito-Garagorri, D.; Puchberger, M.; Mereiter, K.; Kirchner, K. *Angew. Chem., Int. Ed.* **2008**, *47*, 9142.

(14) Allen, F. H. *Acta Crystallogr.* **2002**, *B58*, 380.

(15) See the Supporting Information for more details.

(16) Boro, B. J.; Duesler, E. N.; Goldberg, K. I.; Kemp, R. A. *Inorg. Chem.* **2009**, *48*, 5081.

(17) For complexes **5a**, **5b**, and **6a**, a second relatively strong stretch was observed in the region of the IR spectra where CO stretches are normally observed. Given that pure samples, which had completely isomerized to one product, were used to obtain the IR data, it is unclear what is reponsbile for these stretches. One possibility is that the CO stretch is partially coupled to an Fe−H or B−H stretch, resulting in two vibrations in this region. In all three cases, the stronger stretch has been assigned as ν_{CO}.

(18) Crabtree, R. H. *The Organometallic Chemistry of the Transition Metals*, 5th ed.; Wiley: New York, 2009.

(19) Bondi, A. *J. Phys. Chem.* **1964**, *68*, 441.

(20) (a) Baker, M. V.; Field, L. D. *J. Chem. Soc., Chem. Commun.* **1984**, 996. (b) Baker, M. V.; Field, L. D. *Appl. Organomet. Chem.* **1990**, *4*, 543.

(21) Müller, P. Hydrogen Atoms. In *Crystal Structure Refinement: A Crystallographer's Guide to SHELXL*; Müller, P., Ed.; Oxford University Press: Oxford, U.K., 2006; p 26.

(22) Abdur-Rashid, K.; Graham, T.; Tsang, C.-W.; Chen, X.; Guo, R.; Jia, W.; Amoroso, D.; Sui-Seng, C. (Kanata Chemical Technologies Inc., Canada). The Generation of Hydrogen from Ammonia Borane through Catalytic Hydrolysis. WO 2008141439 A1, 2008.

(23) Grönberg, K. L. C.; Henderson, R. A.; Oglieve, K. E. *J. Chem. Soc., Dalton Trans.* **1998**, 3093.

(24) *CrystalClear and CrystalStructure*; Rigaku/MSC: The Woodlands, TX, 2010.

(25) Altomare, A.; Cascarano, G.; Giacovazzo, C.; Guagliardi, A.; Burla, M. C.; Polidori, G.; Camalli, M. *J. Appl. Crystallogr.* **1994**, *27*, 435.

(26) Sheldrick, G. M. *Acta Crystallogr., Sect. A* **2008**, *64*, 112.

(27) *SHELXTL NT 6.12*; Bruker AXS Inc.: Madison, WI, 2002.

dx.doi.org/10.1021/ic402762v | *Inorg. Chem.* XXXX, XXX, XXX−XXX